Edge Solitons in Nonlinear-Photonic Topological Insulators

Daniel Leykam[1] and Y. D. Chong[1,2]
[1]Division of Physics and Applied Physics, School of Physical and Mathematical Sciences, Nanyang Technological University, Singapore 637371, Singapore
[2]Centre for Disruptive Photonic Technologies, Nanyang Technological University, Singapore 637371, Singapore
(Received 13 June 2016; published 28 September 2016)

We show theoretically that a photonic topological insulator can support edge solitons that are strongly self-localized and propagate unidirectionally along the lattice edge. The photonic topological insulator consists of a Floquet lattice of coupled helical waveguides, in a medium with local Kerr nonlinearity. The soliton behavior is strongly affected by the topological phase of the linear lattice. The topologically nontrivial phase gives a continuous family of solitons, while the topologically trivial phase gives an embedded soliton that occurs at a single power and arises from a self-induced local nonlinear shift in the intersite coupling. The solitons can be used for nonlinear switching and logical operations, functionalities that have not yet been explored in topological photonics. We demonstrate using solitons to perform selective filtering via propagation through a narrow channel, and using soliton collisions for optical switching.

DOI: 10.1103/PhysRevLett.117.143901

Topologically nontrivial photonic bands, analogous to electronic topological insulators, have now been realized and studied in a variety of photonic structures [1–10]. These "photonic topological insulators" (PTIs) feature edge states that are topologically protected against certain classes of disorder, and they have interesting potential applications as robust waveguides and delay lines. Thus far, PTIs have mostly been studied in the linear limit, in which existing concepts of band topology can be directly applied to the electromagnetic wave equations, such as by mapping the propagation equations for a linear-photonic lattice to the linear Schrödinger equation [6]. Even recent studies of PTIs arising in optically nonlinear systems, such as exciton polaritons in quantum wells, have focused on topological edge states that are linear perturbations around a steady-state nonlinear background [11–13]. There have been only a handful of investigations into the *nonperturbative* nonlinear dynamics that could arise in PTIs [14–18]. Notably, Lumer *et al.* discovered a localized stationary soliton lying in the bulk of a two-dimensional (2D) PTI, which can be interpreted as a point region of a different topological phase that is "self-induced" by topological edge states circulating around it [14]. Ablowitz *et al.* have found evidence for moving edge solitons in weakly nonlinear 2D PTIs, though this was done by taking broad envelope superpositions of existing topological edge states, and reducing the system to a 1D nonlinear Schrödinger equation [15]. In 1D lattices, nonlinear dynamics of boundary states and self-induced topological transitions have also been studied [16,17].

This Letter describes a class of moving lattice edge solitons that arise in experimentally feasible 2D PTIs with Kerr nonlinearity. Unlike in Ref. [15], the solitons are derived *ab initio*, without using broad envelope approximations, in a realistic photonic lattice; furthermore, they can arise whether the underlying lattice is topologically trivial or nontrivial in the linear limit. The underlying topological phase strongly affects the soliton properties. In the topologically trivial phase, where the linear lattice lacks topological edge states, the solitons are topologically self-induced, similar to the stationary solitons found in Ref. [14], except that these can move unidirectionally along the edge. They appear to be "embedded" lattice solitons, meaning that they coexist with extended linear modes without being stabilized by a gap [19–21]; the soliton solution occurs at a single power, at which the radiative loss via coupling to small-amplitude linear waves happens to vanish. We note that the only embedded lattice solitons experimentally observed so far have been stationary [22]; well-localized moving lattice solitons are predicted to exist based on discrete models [20,23,24], but they have been challenging to realize experimentally. On the other hand, when the underlying lattice is topologically nontrivial, moving edge solitons occur over a continuous range of powers and are stabilized by the dispersion features of the linear topological edge modes.

The existence of strongly localized moving solitons opens up a range of interesting possibilities for performing signal processing in PTI lattices [25], beyond what could be accomplished using linear topological edge states or stationary solitons [14]. We present two representative examples: (i) self-focusing of edge modes, allowing them to be "squeezed" through narrow channels without backreflection, and (ii) collisions between edge and bulk solitons, which can be used for all-optical signal switching.

The photonic lattice, shown schematically in Fig. 1(a), consists of a 2D square lattice of helical waveguides,

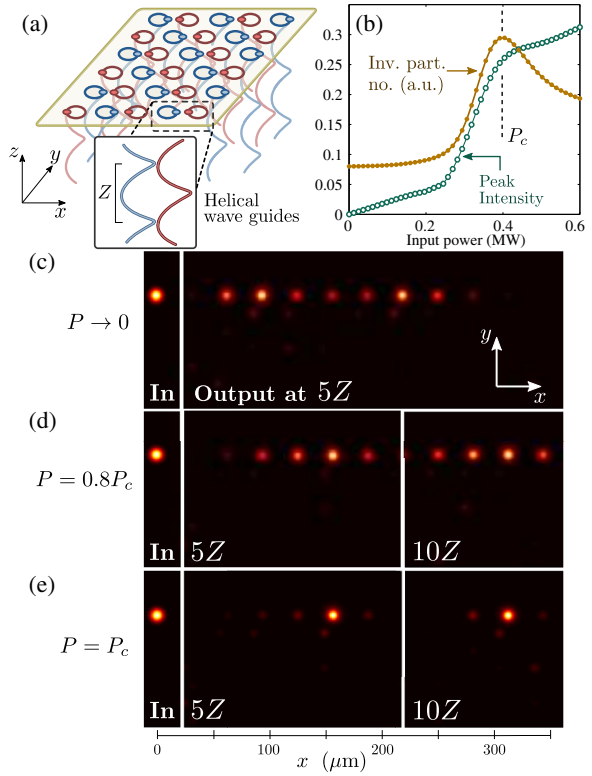

FIG. 1. (a) Schematic of a photonic lattice of helical waveguides forming a square lattice in the $x-y$ plane. On each sublattice (red and blue; right and left in inset respectively), the helix phase is staggered by π. (b)–(e) Beam propagation simulation results showing solitonic self-focusing in a topologically nontrivial lattice. The lattice consists of a strip four lattice constants wide, with single-site input on the edge at $z = 0$. (b) Peak intensity $I_{\max}$ and inverse participation number $\mathcal{P}^{-1}$ at $z = 5Z$ (i.e., after five helix cycles), versus input power P. Corresponding in-plane intensity profiles at various propagation distances, for (c) $P \to 0$, (d) $P = 0.8P_c$, and (e) $P = P_c$, where P_c is the power at which the soliton is most localized (i.e., $\mathcal{P}^{-1}$ is the largest).

"staggered" so that neighboring waveguides (in different sublattices) have helix phase shifts of π relative to each other; hence, each waveguide approaches its four neighbors sequentially during each helix cycle [26]. The waveguides are otherwise identical. In the linear optics regime, we have previously shown that the photonic band structure can be either topologically trivial (a conventional insulator) or nontrivial (an anomalous Floquet PTI), depending on the interwaveguide couplings [26]. Now, we include a local Kerr nonlinearity in the optical medium. In the paraxial approximation, the propagation of a monochromatic beam envelope $\psi(x, y, z)$ obeys

$$i\partial_z\psi = -\frac{1}{2k_0}\nabla_\perp^2\psi - \frac{k_0}{n_0}(n_L(x, y, z) + n_2|\psi|^2)\psi. \qquad (1)$$

This is a nonlinear Schrödinger equation with the axial coordinate z playing the role of time; $k_0 = 2\pi n_0/\lambda$ is the wave number, $\nabla_\perp^2 \equiv \partial_x^2 + \partial_y^2$ is the transverse Laplacian operator, n_0 is the background refractive index, and n_L and $n_2|\psi|^2$ are the linear and nonlinear local refractive index deviations from n_0. The function $n_L(x, y, z)$ corresponds to the helix lattice described above, with mean waveguide spacing a, helix radius R_0, and modulation period Z. We adopt parameter values consistent with fused silica glass at wavelength $\lambda = 1550$ nm: $n_0 = 1.45$, $n_L \sim 2.7 \times 10^{-3}$ in the waveguides (and $n_L = 0$ outside), and $n_2 = 3 \times 10^{-20}$ m^2/W [27] (self-focusing nonlinearity; a defocusing nonlinearity can give rise to similar effects [28]). The waveguides have circular cross sections with radius 4 μm. The paraxial beam intensity $|\psi|^2$ is normalized by the characteristic intensity $I_0 = 10^{16}$ W/m^2, for which the nonlinear index shift $n_2 I_0$ is comparable to n_L. For the modal area of one waveguide, $w_0^2 \sim (10\ \mu\text{m})^2$, this requires peak powers $\sim$1 MW, accessible with pulsed lasers [27].

In the linear regime ($n_2 \to 0$), the Floquet eigenmodes of the system can be obtained by solving

$$\hat{U}(Z)\psi = \exp\left[-i\int_0^Z \hat{H}(z)dz\right]\psi = e^{-i\beta Z}\psi, \qquad (2)$$

where $\hat{H}$ is the Hamiltonian in Eq. (1), and β is the Floquet quasienergy defined modulo $2\pi/Z$ [6,26,31–33]. The topology of the Floquet band structure is governed by an effective coupling angle $\theta_0 \in [0, \pi]$ controlling the band gap size, with the system topologically nontrivial when $0.25\pi < \theta_0 < 0.75\pi$ [26,28].

We use beam propagation simulations of Eq. (1) to study nonlinear waves produced by injecting light at the edge of a semi-infinite strip. First, consider a lattice that is topologically nontrivial in the linear limit, with coupling angle $\theta_0 = 0.6\pi$ (from helix parameters $a = 22$ μm, $R_0 = 4$ μm, and $Z = 1$ cm). When the input power P is very low, the initial single-site excitation couples to linear topological edge states. As shown in Fig. 1(c), this produces a wave packet propagating in one direction along the edge (since the edge states are unidirectional) while undergoing broadening (since the dispersion of the edge states is not perfectly linear [26]). Upon increasing P, the Kerr nonlinearity induces self-focusing, and we observe solitonic propagation along the edge of the lattice, as shown in Figs. 1(d) and 1(e). We momentarily put aside the issue of soliton stability, which will be discussed below. To quantify the self-focusing, Fig. 1(b) plots the peak intensity $I_{\max} = \max(|\psi|^2)$ and the inverse participation number $\mathcal{P}^{-1} = \int|\psi|^4 dxdy/(\int|\psi|^2 dxdy)^2$, after propagation through five helix cycles. At a critical power P_c, the soliton becomes localized to almost a single site, as shown in Fig. 1(e). This self-focusing effect does not appear to be describable using a purely on-site nonlinearity of the sort used in Refs. [14,15], but it can be modeled by a nonlinear shift in the effective coupling angle [34,35]:

$$\theta_{\text{eff}} \approx \theta_0 - \theta_{\text{NL}}|\psi|^2. \quad (3)$$

In previously studied discrete nonlinear lattice models, similar coupling nonlinearities were shown to produce "compact" solitons that are perfectly localized to a few sites [36,37]. In our photonic lattice, the shift is due to the self-focusing Kerr nonlinearity increasing the waveguide depth, thus reducing the evanescent interwaveguide coupling. When $P = P_c$, the coupling angle reaches $\theta_{\text{eff}} = 0.5\pi$, which corresponds to perfect coupling into neighboring waveguides at each quarter cycle of the helix. This is the "middle" of the topological insulator phase, where the edge states are maximally localized.

We now turn to a lattice that is topologically trivial in the linear limit. As shown in Figs. 2(a) and 2(b), injecting light at the edge of the nonlinear lattice at a certain input power can produce a strongly localized moving soliton. Since the linear lattice in this case lacks topological edge states, the soliton in Fig. 2(b) is "topologically self-induced": the field intensity near the soliton drives the local region of the lattice from the topologically trivial phase to the nontrivial phase via Eq. (3). Here, the linear lattice has the coupling angle $\theta_0 = 0.9\pi$ (from helix parameters $a = 25$ μm, $R_0 = 6$ μm, and $Z = 2$ cm), and the nonlinearity drives the local coupling angle below the topological transition located at $\theta = 0.75\pi$. Unlike the topologically self-induced stationary solitons observed in Ref. [14] (in a nonstaggered helical lattice), these solitons are mobile, and they move unidirectionally along the edge.

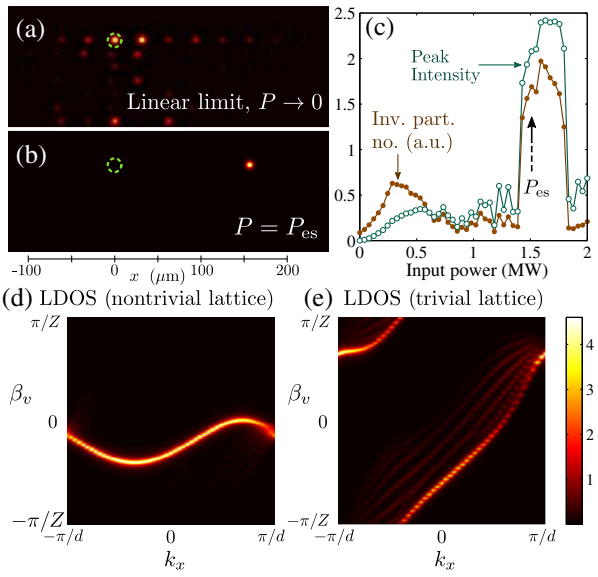

FIG. 2. Self-induced nonlinear edge modes in a topologically trivial lattice. (a),(b) Intensity profiles after propagation through $z = 5Z$, starting from a single-site excitation (the dotted circle), for (a) the zero-power (linear) limit $P \to 0$, and (b) input power P_{es} corresponding to the embedded soliton. (c) Peak intensity I_{max} and inverse participation ratio $\mathcal{P}^{-1}$ at $z = 5Z$, versus input power P. (d),(e) Local density of states along the edge, for the nontrivial and trivial lattices in the linear limit, plotted using the moving-frame quasienergies defined by $\beta_v(k_x) \equiv \beta(k_x) - vk_x$.

In contrast to the solitons found in the nontrivial lattice, the soliton in Fig. 2(b) is only observed near a specific input power P_{es}. Figure 2(c) plots the peak intensity and inverse participation number versus the input power P. Both quantities are strongly suppressed except near $P_{\text{es}} \approx 1.5$ MW. For other values of P, the input light diffracts strongly into the bulk, and the wave packet decays with z until the nonlinearity becomes negligible [38].

The stability of a soliton depends on whether there exist small-amplitude linear waves that the soliton can decay into. For stable propagation at velocity v, the soliton must avoid resonance with linear waves in its moving frame, whose quasienergies are $\beta_v(k_x) \equiv \beta(k_x) - vk_x$ [20]. In Figs. 2(d) and 2(e), we plot the moving-frame local density of states (LDOS) on the lattice edge. For the previous topologically nontrivial lattice (corresponding to the results shown in Fig. 1), we see from Fig. 2(d) that the LDOS is dominated by the linear topological edge states (the bulk states' contribution is about 1% of the bulk contribution in the trivial lattice). Since the edge states are unidirectional and have nearly linear dispersion, they only occupy a narrow range of β_v. This allows soliton families to avoid resonating with linear modes [15]. In the topologically trivial lattice, however, there is significant LDOS for all β_v's because the contributing bulk modes are not unidirectional. Thus, a traveling edge wave is typically destabilized by decaying into small-amplitude bulk modes. As an exception, at a specific power P_{es}, coupling to the bulk modes could vanish, leading to the formation of an "embedded soliton" [19–21]. This explains the semistable behavior shown in Figs. 2(b) and 2(c): embedded solitons typically have a finite basin of attraction, so, for $P \gtrsim P_{\text{es}}$, the excess energy is radiated away, but if P is too large, the wave packet fails to relax to the soliton.

To further verify that these are soliton solutions, we formulated a discrete model for the photonic lattice and searched for nonlinear modes using the Floquet self-consistency method developed in Ref. [14]. In the nontrivial lattice, the procedure converged numerically to solutions corresponding to moving solitons on the edge, as well as stationary gap solitons in the bulk. In the trivial lattice, we obtained convergence to an embedded moving soliton localized to a single site and verified that its power can be described by $P_{\text{es}} \approx (\theta_0 - \pi/2)/\theta_{\text{NL}}$. Details are given in the Supplemental Material [28].

Another practical constraint on soliton stability comes from bending losses, i.e., radiation into nonlattice modes. For the chosen helical waveguide parameters, bending losses for the linear topological edge states are very low, on the order of 1% per helix cycle [26]. Figure 3(a) shows the power retained on the edge waveguides with an increasing z. In the nontrivial lattice, after an initial power-dependent transient oscillation (caused by the choice

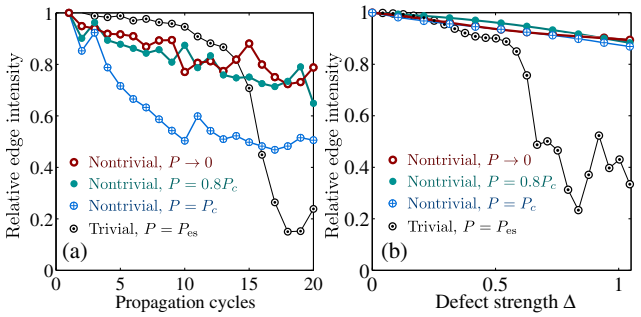

FIG. 3. Stability of nonlinear edge modes in trivial and nontrivial photonic lattices. (a) Relative edge intensity (the ratio of the edge intensity to the initial edge intensity at $z = 0$) versus propagation distance z. (b) Relative edge intensity at $z = 5Z$, after scattering off a defect with the normalized strength $\Delta \equiv \delta n k_0 Z/(2\pi n_0)$, where δn is the detuning of the defect waveguide's refractive index.

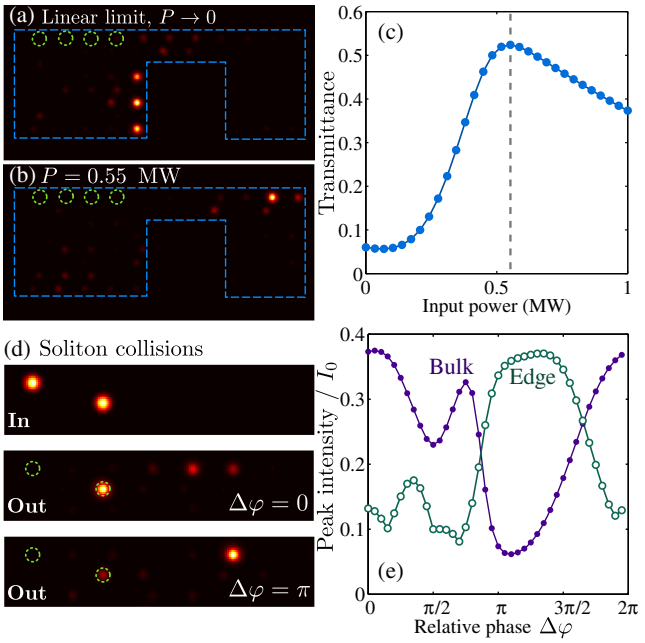

FIG. 4. Nonlinear filtering and switching using edge solitons. (a)–(c) Power-dependent filtering by a narrow channel. The intensity profile at $z = 8Z$ is plotted for (a) the linear limit $P \to 0$ and (b) the nonlinear regime at $P = 0.55$ MW. The input light is injected uniformly on four waveguides marked by green circles, and the lattice boundary is marked by blue dashes. (c) Transmittance through the channel (defined as the total intensity on the edge sites to the right of the channel) versus input power P. (d),(e) Optical switching by bulk-edge soliton collisions. (d) Intensity profiles at $z = 0$ before the collision, and at $z = 5Z$ after the collision. (e) Postcollision peak intensities in the bulk and edge waveguides versus the relative phase $\Delta\varphi$ of the inputs.

of single-waveguide excitation), the solitons have decay rates comparable to the linear topological edge states. In the trivial lattice, however, the soliton abruptly destabilizes after ~15 cycles due to bending losses reducing the power below P_{es} and triggering a breakup.

We now ask how robust the solitons are against defects and lattice shape deformations. Topological edge states of linear PTIs are known to be highly robust, limited mainly by finite-size effects (i.e., scattering to the opposite edge) and losses [9,26], so long as the paraxial limit (or any other assumption responsible for topological protection) holds. In Fig. 3(b), we study the effects of a defect formed by detuning the depth of a single waveguide on the edge. In the nontrivial lattice, the robustness of the solitons is found to be comparable to the linear edge states. In the trivial lattice, the soliton survives for small defect strengths, but sufficiently strong defects cause it to abruptly destabilize (by leaving the "stability band" around P_{es}). The embedded solitons are thus inherently less robust than the linear topological edge states and the solitons of the nontrivial lattice. On the other hand, both soliton types are robust against changes in the lattice shape; they are able to move around corners and missing sites without backscattering, and with much less dispersion compared to the edge states of the linear PTI [28].

We conclude with two examples of using solitons to perform nonlinear filtering and switching. These will use the solitons of the nontrivial lattice due to their greater stability. In Figs. 4(a)–4(c), we show how a narrow channel can act as a power-dependent filter. The channel is one unit cell wide, connecting two wider strips. In the linear regime [Fig. 4(a)], the edge states fail to pass through the channel and are instead diverted, because topological protection is lost when there is a significant spatial overlap of modes on opposite edges. Increasing the input power P [Fig. 4(b)] causes the formation of a soliton that is sufficiently strongly localized to pass through the channel. As shown in Fig. 4(c), the transmittance exhibits an 8.6-fold variation as P goes from 0 to 0.55 MW.

Next, Figs. 4(d) and 4(e) shows how a collision between a moving edge soliton and a stationary gap soliton can function as a nonlinear optical switch. The stationary gap soliton is produced by exciting a waveguide one unit cell away from the edge [28]. The two solitons are initialized with the relative phase $\Delta\varphi$, and both have input power $P = P_c$ for which the soliton is maximally localized (see Fig. 1). We find that the result of the collision depends strongly on $\Delta\varphi$ [39,40]. Figure 4(e) shows how the peak intensities on the edge and bulk sites, at $z = 5Z$ after the collision, vary with $\Delta\varphi$. Certain choices of $\Delta\varphi$ allow us to almost completely destroy one of the solitons.

In summary, we predict the existence of strongly localized, mobile, and unidirectional edge solitons in experimentally feasible 2D photonic topological insulator lattices with Kerr nonlinearities. Like topological edge states, the solitons move unidirectionally and can bypass corners and missing-site defects without backscattering. The solitons in the nontrivial lattice inherit some of the linear edge states' robustness against perturbations such as

waveguide detunings. The trivial lattice supports topologically self-induced embedded solitons, which are unstable against perturbations and bending losses. We have studied two simple examples of using solitons for nonlinear filtering and switching. In future work, it would be interesting to explore, using these solitons for nontrivial signal processing tasks, to determine whether the topological lattice design confers practical advantages over previously studied solitonic lattices, and to look for similar nonlinear modes in other photonic, polaritonic, or phononic lattices.

We are grateful to T. C. H. Liew, M. C. Rechtsman, C. Soci, and B. Zhang for the helpful discussions. This research was supported by the Singapore National Research Foundation under Grant No. NRFF2012-02, and by Singapore MOE Academic Research Fund Tier 2 Grant No. MOE2015-T2-2-008.

[1] L. Lu, J. D. Joannopoulos, and M. Soljačić, Topological photonics, Nat. Photonics **8**, 821 (2014).
[2] F. D. M. Haldane and S. Raghu, Possible Realization of Directional Optical Waveguides in Photonic Crystals with Broken Time-Reversal Symmetry, Phys. Rev. Lett. **100**, 013904 (2008).
[3] S. Raghu and F. D. M. Haldane, Analogs of quantum-Hall-effect edge states in photonic crystals, Phys. Rev. A **78**, 033834 (2008).
[4] Z. Wang, Y. Chong, J. D. Joannopoulos, and M. Soljačić, Observation of unidirectional backscattering-immune topological electromagnetic states, Nature (London) **461**, 772 (2009).
[5] A. B. Khanikaev, S. H. Mousavi, W.-K. Tse, M. Kargarian, A. H. MacDonald, and G. Shvets, Photonic topological insulators, Nat. Mater. **12**, 233 (2013).
[6] M. C. Rechtsman, J. M. Zeuner, Y. Plotnik, Y. Lumer, D. Podolsky, F. Dreisow, S. Nolte, M. Segev, and A. Szameit, Photonic Floquet topological insulators, Nature (London) **496**, 196 (2013).
[7] M. Hafezi, S. Mittal, J. Fan, A. Migdall, and J. M. Taylor, Imaging topological edge states in silicon photonics, Nat. Photonics **7**, 1001 (2013).
[8] A. P. Slobozhanyuk, A. B. Khanikaev, D. S. Filonov, D. A. Smirnova, A. E. Miroshnichenko, and Y. S. Kivshar, Experimental demonstration of topological effects in bianisotropic metamaterials, Sci. Rep. **6**, 22270 (2016).
[9] F. Gao, Z. Gao, X. Shi, Z. Yang, X. Lin, J. D. Joannopoulos, M. Soljačić, H. Chen, L. Lu, Y. Chong, and B. Zhang, Probing the limits of topological protection in a designer surface plasmon structure, Nat. Commun. **7**, 11619 (2016).
[10] S. Mukherjee *et al.*, Experimental observation of anomalous topological edge modes in a slowly-driven photonic lattice, arXiv:1604.05612; L. C. Maczewsky, J. M. Zeuner, S. Nolte, and A. Szameit, Observation of photonic anomalous Floquet topological insulators, arXiv:1605.03877.
[11] C.-E. Bardyn, T. Karzig, G. Refael, and T. C. H. Liew, Chiral Bogoliubov excitations in nonlinear bosonic systems, Phys. Rev. B **93**, 020502(R) (2016).
[12] V. Peano, M. Houde, C. Brendel, F. Marquardt, and A. A. Clerk, Topological phase transitions and chiral inelastic transport induced by the squeezing of light, Nat. Commun. **7**, 10779 (2016).
[13] B. Galilo, D. K. K. Lee, and R. Barnett, Selective Population of Edge States in a 2D Topological Band System, Phys. Rev. Lett. **115**, 245302 (2015).
[14] Y. Lumer, Y. Plotnik, M. C. Rechtsman, and M. Segev, Self-Localized States in Photonic Topological Insulators, Phys. Rev. Lett. **111**, 243905 (2013).
[15] M. J. Ablowitz, C. W. Curtis, and Y.-P. Ma, Linear and nonlinear traveling edge waves in optical honeycomb lattices, Phys. Rev. A **90**, 023813 (2014).
[16] Y. Hadad, A. B. Khanikaev, and A. Alu, Self-induced topological transitions and edge states supported by nonlinear staggered potentials, Phys. Rev. B **93**, 155112 (2016).
[17] Y. Gerasimenko, B. Tarasinski, and C. W. J. Beenakker, Attractor-repeller pair of topological zero-modes in a nonlinear quantum walk, Phys. Rev. A **93**, 022329 (2016).
[18] Y. Lumer, M. C. Rechtsman, Y. Plotnik, and M. Segev, Instability of bosonic topological edge states in the presence of interactions, Phys. Rev. A **94**, 021801(R) (2016).
[19] A. R. Champneys, B. A. Malomed, J. Yang, and D. J. Kaup, Embedded solitons: Solitary waves in resonance with the linear spectrum, Physica D (Amsterdam) **152D**, 340 (2001).
[20] T. R. O. Melvin, A. R. Champneys, P. G. Kevrekidis, and J. Cuevas, Radiationless Traveling Waves in Saturable Nonlinear Schrödinger Lattices, Phys. Rev. Lett. **97**, 124101 (2006).
[21] J. Fujioka, A. Espinosa-Cerón, and R. F. Rodríguez, A survey of embedded solitons, Rev. Mex. Fis. **52**, 6 (2006).
[22] X. Wang, Z. Chen, J. Wang, and J. Yang, Observation of In-Band Lattice Solitons, Phys. Rev. Lett. **99**, 243901 (2007).
[23] D. E. Pelinovsky and V. M. Rothos, Bifurcations of travelling wave solutions in the discrete NLS equations, Physica D (Amsterdam) **202D**, 16 (2005).
[24] B. A. Malomed, J. Fujioka, A. Espinosa-Cerón, R. F. Rodríguez, and S. González, Moving embedded lattice solitons, Chaos **16**, 013112 (2006).
[25] D. N. Christodoulides and E. D. Eugenieva, Blocking and Routing Discrete Solitons in Two-Dimensional Networks of Nonlinear Waveguide Arrays, Phys. Rev. Lett. **87**, 233901 (2001).
[26] D. Leykam, M. C. Rechtsman, and Y. D. Chong, Anomalous Topological Phases and Unpaired Dirac Cones in Photonic Floquet Topological Insulators, Phys. Rev. Lett. **117**, 013902 (2016).
[27] A. Szameit, J. Burghoff, T. Peertsch, S. Nolte, A. Tünnermann, and F. Lederer, Two-dimensional soliton in cubic fs laser written waveguide arrays in fused silica, Opt. Express **14**, 6055 (2006).
[28] See Supplemental Material at http://link.aps.org/supplemental/10.1103/PhysRevLett.117.143901, which includes Refs. [29,30], for further simulations and analysis of the nonlinear tight binding model.
[29] E. Yeganegi, A. Lagendijk, A. P. Mosk, and W. L. Vos, Local density of optical states in the band gap of a finite one-dimensional photonic crystal, Phys. Rev. B **89**, 045123 (2014).

[30] S. Raghavan, A. Smerzi, S. Fantoni, and S. R. Shenoy, Coherent oscillations between two weakly coupled Bose-Einstein condensates: Josephson effects, π oscillations, and macroscopic quantum self-trapping, Phys. Rev. A **59**, 620 (1999).

[31] T. Kitagawa, E. Berg, M. Rudner, and E. Demler, Topological characterization of periodically driven quantum systems, Phys. Rev. B **82**, 235114 (2010).

[32] M. S. Rudner, N. H. Lindner, E. Berg, and M. Levin, Anomalous Edge States and the Bulk-Edge Correspondence for Periodically Driven Two-Dimensional Systems, Phys. Rev. X **3**, 031005 (2013).

[33] M. Pasek and Y. D. Chong, Network models of photonic Floquet topological insulators, Phys. Rev. B **89**, 075113 (2014).

[34] S. M. Jensen, The nonlinear coherent coupler, IEEE Trans. Microwave Theory Tech. **30**, 1568 (1982).

[35] P. R. Berger, P. K. Bhattacharya, and S. Gupta, A waveguide directional coupler with a nonlinear coupler medium, IEEE J. Quantum Electron. **27**, 788 (1991).

[36] P. G. Kevrekidis, V. V. Konotop, A. R. Bishop, and S. Takeno, Discrete compactons: Some exact results, J. Phys. A **35**, L641 (2002).

[37] M. Öster and M. Johansson, Stability,mobility and power currents in a two-dimensional model for waveguide arrays with nonlinear coupling, Physica D (Amsterdam) **238D**, 88 (2009).

[38] A. Szameit, Y. V. Kartashov, F. Dreisow, T. Pertsch, S. Nolte, A. Tünnermann, and L. Torner, Observation of Two-Dimensional Surface Solitons in Asymmetric Waveguide Arrays, Phys. Rev. Lett. **98**, 173903 (2007).

[39] G. I. Stegeman and M. Segev, Optical spatial solitions and their interactions: Universality and diversity, Science **286**, 1518 (1999).

[40] J. Cuevas and J. C. Eilbeck, Discrete soliton collisions in a waveguide array with saturable nonlinearity, Phys. Lett. A **358**, 15 (2006).